Diffusion of Polystyrene Solutions through Model Membranes. 1. Diffusion Kinetics of Monodisperse Solutions

G. Guillot

Physique de la Matière Condensée,† Collège de France, 75231 Paris Cedex 05, France.
Received June 27, 1986

ABSTRACT: The diffusion of monodisperse solutions of polystyrene molecules through model porous membranes of pore radius R_p = 75 nm has been examined as a function of the polymer concentration and of the membrane porosity. Experiments conducted under different porosities are compared. It is shown that diffusional boundary layers may become of importance with high-porosity filters. The concentration dependence of the diffusion kinetics has been investigated for two molecular weights. The short chains (molecular weight $m_w = 8.7 \times 10^5$) have a hydrodynamic radius r_H = 24 nm, smaller than R_p, and their diffusion kinetics across the membrane is a moderately increasing function of concentration. In contrast, the long chains (molecular weight $M_w = 6.77 \times 10^6$) have a hydrodynamic radius R_H = 60 nm, comparable to R_p. Their diffusion across the membrane is strongly hindered in dilute solution and drastically accelerated at concentrations higher than their first overlap concentration c^*_M. This enhanced diffusion may be attributed to the concentration dependence of the partition coefficient between pores and outside solution. The results can be qualitatively well described by using a scaling approach. However, a simple virial expansion is also in good agreement with our data and with previous evaluations of the virial coefficient in the solutions under investigation (polystyrene in ethyl acetate).

Introduction

Transport of macromolecular solutes through porous media is involved in various experimental situations (ultrafiltration, gel permeation chromatography) and is now routinely used in enhanced oil recovery.

It is usually considered that the size of the solute as compared to the pore size controls the entrance of the solute into the porous media. Indeed, experimental data on diffusion or flow of rigid solutes and small molecular weight polymers well support this view in a variety of porous materials: leached Vycor glass[1,2] or track-etched membranes with cylindrical pores.[3-5,29] These results are in fair agreement with simple hydrodynamic models for the restricted transport of rigid solutes in neutral porous media.[6-9] The more sophisticated calculation of the partition coefficient K (ratio of the concentration inside the pore to the outside concentration) for ideal flexible chains at infinite dilution by Casassa[10] uses a statistical analysis of the polymer conformation. The dependence of K on chain size is similar with this analysis or one using a hard sphere model for chains small as compared to the pore size.

However, flexible chains should also penetrate pores smaller than their hydrodynamic radius, in contrast to rigid particles. Such a behavior has been observed with Vycor glass[11] as well as track-etched membranes.[4a,5,12] Moreover, the transport of flexible chains is also increased when either flow rate[13,14] or concentration[15,16] are increased. Using the scaling description of semidilute polymer solutions, Daoudi and Brochard have shown that in the absence of flow long flexible chains should enter into small pores without exclusion at high enough concentration:[17] when the presence of neighboring chains screens the excluded volume and hydrodynamic interactions down to distances smaller than the pore size,[18] the partition coefficient should become comparable to 1.

Large chains excluded from small pores in dilute conditions are then expected to present an increase of their partition coefficient with concentration. We recently reported data on the concentration dependence of the diffusion rate of large flexible chains in the absence of flow through track-etched membranes of well-defined geometry (porosity, thickness, and pore radius).[16]

In the present paper, new data of similar experiments are reported. The results are also compared to a more elaborated model than in ref 16. We examine the concentration dependence of the diffusion kinetics for two molecular weights and two porosities. The observed acceleration of diffusion is compared to the variation of the partition coefficient when interchain interactions are taken into account, from the dilute regime up to the semidilute one. We use virial coefficients known from different independent studies of the same solutions, polystyrene in ethyl acetate,[19,20] for comparison with our own data.

In an accompanying paper, we examine the diffusion kinetics for bimodal solutions of the same two molecular weights, as a function of polymer concentration and solution composition in long and short chains.[21]

Experimental Section

A. Membranes. Membrane preparation and characterization have been described elsewhere in more detail.[16-22] Latent tracks are formed in polycarbonate films by heavy ion irradiation (Kr^{25+} ions accelerated at 6 MeV/N) performed in A.L.I.C.E. synchrotron in Orsay. These tracks are later etched by a sodium hydroxyde solution to produce cylindrical pores spanning the membrane. The pore density is fixed by the irradiation does and the pore radius is governed by the duration of the etching.

The membranes have been observed with a scanning electron microscope after deposition of a thin metallic layer to evaluate the pore density, the pore size, and the pore size distribution. For $R_p > 50$ nm, the pore shape is very regular and the pore size distribution appears very narrow but for $R_p < 50$ nm, the pore size is very inhomogeneous, probably because of the partial crystallinity of the polycarbonate samples (Makrofol KG and N from Bayer). Two other techniques have been more routinely used to characterize the membrane, conductivity and permeability: the conductance of the membrane soaked in an electrolyte solution is proportional to the overall pore area and provides a value of $\langle R_p^2 \rangle$ if the pore density is separately known; under the same condition, the measurement of the flow rate under constant pressure in Poiseuille flow conditions gives $\langle R_p^4 \rangle$. The pore sizes obtained by these techniques are systematically larger than the pore sizes observed in SEM, by about 20 nm. No consistent explanation for this discrepancy is available. Since there is a close agreement (within 2%) between the two macroscopic measurements for $R_p > 50$ nm, we infer that the pore size distribution is narrow and we use for the R_p value the data of conductivity or permeability.

All the diffusion experiments were conducted with membranes of comparable geometrical characteristics: membrane thickness L = 10 μm, pore radius R_p = 75 nm, and total number of pores $N_p = 8 \times 10^8$ on a surface 1 cm^2. Such a high porosity p (p = 14%) was chosen to shorten the duration of the diffusion experiments. It was easily checked that no macroscopic tearing had

† Unité Associée au CNRS (U.A. 792).

0024-9297/87/2220-2600$01.50/0

occurred on either membrane through the order of magnitude of the times characterizing the diffusion of the polymer molecules.

It has been checked that the solvent chosen, ethyl acetate, does not alter the membrane properties and that there is no adsorption of polymer on the membranes (16).

B. Solutions. We have prepared by weighing polystyrene solutions of the two molecular weights $M_w = 6.77 \times 10^6$ and $m_w = 8.7 \times 10^5$ in freshly distilled ethyl acetate. The solutions are prepared in advance and they are allowed to homogenize by gentle intermittent stirring for 2 or 3 weeks prior to a diffusion experiment.

The large molecular weight has the same origin as in ref 16, it is a commercial sample of Toyosoda (grade F-700). Its polydispersity as given by the manufacturer is $I = 1.14$. We have used for the small molecular weight sample polystyrene labeled with spiropyran synthetized by Professor Rempp in Strasbourg. After anionic preparation, the living polymer has been divided into two parts, one was deactivated with methanol to give unlabeled chains, the other was deactivated with a solution of spiropyran molecules to give polystyrene chains with one spiropyran molecule at each extremity.[23] Labeled and unlabeled chains of this polystyrene have been characterized by gel permeation chromatography.[24] The unlabeled chain molecular weight is 6.2×10^5 and their polydispersity index 1.2. The labeled chains' distribution is much broader and presents two maxima at 6×10^5 and 1.2×10^6; this bimodal distribution is probably due to duplications that occurred during the spiropyran labeling process. The weight-average molecular weight of the labeled chains is then larger: $m_w = 8.7 \times 10^5$ and their polydispersity index $I = 1.4$.

The hydrodynamic radius of the chains has been determined by quasi-elastic light scattering performed under dilute conditions:[16] $R_H = 58 \pm 3$ nm for the long (N) chains, and $r_H = 24 \pm 2$ nm for the short (n) chains. We have also observed that for large chains ($M_W > 10^6$), the scaling law, $R_H \propto M_W$ (0.55 ± 0.02), characteristic of good solvent conditions is followed.

C. Diffusion Cell. We have used the same diffusion cell as in ref 16, where it is described in more detail. A porous membrane of 1-cm^2 area separates two compartments of respective volumes V_1 and V_2. These volumes are measured by weighing to a 1% accuracy during the filling of the cell. Typically, $V_1 = 0.8$ cm^3 and $V_2 = 3.2$ cm^3. Both compartments are tightly sealed to prevent solvent evaporation. Compartment 2 is equipped with two quartz windows which permit optical density measurements.

The kinetics of diffusion are followed by absorption spectroscopy. All measurements are done on a spectrophotometer Varian Cary 219 in the double-beam automatic-gain mode. The total polystyrene concentration in compartment 2, c_2, is monitored from the absorption of styrene at 268 nm. Because of the long optical path of the cell (2 cm), the upper limit to an in situ measurement of c_2 is 10^{-3} g/g, corresponding to an optical density of 3.

D. Description of a Diffusion Experiment. Both compartments of the diffusion cell are first carefully rinsed several times with filtered, freshly distilled solvent. Compartment 1 is then filled with a polymer solution at the initial total polystyrene concentration $c_{1,0}$, while compartment 2 is filled with pure solvent. Both compartments are completely filled to ensure constant volume conditions. Under the concentration difference established across the membrane, the polymer chains tend to diffuse, and the total polystyrene concentrations c_1 and c_2 of both compartments evolve toward the equilibrium concentration $c_{eq} = c_{1,0}V_1/(V_1 + V_2)$. Each compartment is constantly homogenized by small magnetic stirring bars, at a stirring rate $f = 80 \pm 20$ rpm, in order to get well-defined limiting conditions for the diffusion. The initial concentration $c_{1,0}$ is determined by absorption spectroscopy at 268 nm in a quartz cuvette of 1-mm optical path to a relative accuracy of ±1.5%. The concentration in compartment 2, c_2, is monitored as a function of time by spectroscopy until $c_2 > 10^{-3}$ g/g.

After 4–10 days, the experiment is interrupted. The concentrations c_1 and c_2 are determined by transferring the solutions in a quartz cuvette of 1-mm optical path and measuring their absorption at 268 nm.

In some cases, successive experiments have been undertaken with the same membrane when the cell was thoroughly rinsed several times after interruption. All the experiments have been performed at room temperature $T \simeq 20$ °C.

Results

A. Diffusion Resistance: Influence of Stirring Conditions. From the evolution of concentration in compartment 2, we have access to the diffusion coefficient through the membrane.

The concentration difference between the two compartments $(c_1 - c_2)$ induces a flow of molecules from compartment 1 to compartment 2. The flux Φ (number of molecules flowing per unit time transported to the membrane surface S) is proportional to $(c_1 - c_2)$ through the resistance to diffusion $\mathcal{R}$: $\Phi\mathcal{R} = (c_1 - c_2)$. The diffusion rate τ^{-1} at which c_2 evolutes toward equilibrium depends on geometrical characteristics of the cell (the volumes V_1 and V_2 of the two compartments and the membrane surface S) and on the resistance: $\mathcal{R} = \tau S[(1/V_1) + (1/V_2)]$. Volume differences may appear between various cells, by 15% for V_1 and 7% for V_2. One should then compare the resistances rather than the times characterizing diffusion kinetics if comparable membranes but various cells are used.

When the boundary condition of a uniform concentration in each compartment is achieved, the resistance to diffusion is only due to the membrane: $\mathcal{R} = \mathcal{R}_m$. The membrane resistance $\mathcal{R}_m$ gives access to the effective diffusion coefficient through the membrane D_{eff}, if the membrane thickness L and the porosity $p = N_p\pi R_p^2/S$ are known: $\mathcal{R}_m = L/(pD_{eff})$.

However, insufficient stirring may build diffusional boundary layers on each side of the membrane, which increase the resistance to diffusion. From the analysis of Malone et al.[25] applicable to the case of dilute solutions, the measured resistance is the sum $\mathcal{R} = \mathcal{R}_m + 2\mathcal{R}_{bl}$. The diffusional boundary layer resistance $\mathcal{R}_{bl} = \delta/D_0$ depends on D_0, the diffusion coefficient of the solute in free solution, and on δ, the boundary layer thickness. δ decreases with the stirring rate and the solute size: $\delta \propto f^{-1/2}D_0^{1/3}$.

We have checked that the kinetics observed with dilute solutions of both types of chains are independent of the stirring rate for 50 rpm $< f <$ 200 rpm within the experimental uncertainty (±10%). This shows that $\mathcal{R}_{bl}$ cannot exceed 20% of $\mathcal{R}_m$. A direct evaluation of δ in a larger range of stirring rate is somewhat delicate to investigate in solutions of large molecules, since too large velocity gradients applied for a prolonged time may induce chain degradation.[26] The ratio $\rho = 2\mathcal{R}_{bl}/\mathcal{R}_m$ or $\rho = (D_{eff}/D_0) \times (2\delta/L)p$ can be also more quantitatively evaluated for solutes that are small as compared to the pore size, for which the importance of the diffusional boundary layer resistance is enhanced ($D_{eff}/D_0 \simeq 1$ and δ is larger).[27] We have observed that the resistance to diffusion of solutions of free spiropyrans ($D_0 = 10^{-5}$ cm^2/s, concentration 5×10^{-4} g/g) decreases by a factor of 2 ± 0.2 as the stirring rate varies from 50 to 500 rpm when membranes of porosity $p = 14\%$ are used.[28] The diffusional boundary layer thickness at $f = 50$ rpm can then be estimated for spiropyran molecules, $\delta_{spiro} \simeq 100$ μm, and by extrapolation to larger solutes ($\delta \propto D_0^{1/3}$), for dilute solutions of both molecular weights, $\delta(m_w = 8.7 \times 10^5) \simeq 30$ μm and $\delta(M_w = 6.77 \times 10^6) \simeq 20$ μm. Since the size of the polystyrene chains is comparable to R_p, we also expect their diffusion to be significantly hindered by the membrane: $D_{eff}/D_0 < 1$. The ratio $\mathcal{R}_{bl}/\mathcal{R}_m$ should then be smaller than 20% for these large molecules, in agreement with our observations on dilute solutions.

B. *n* Chains Alone. The evolution with time of the concentration in compartment 2, c_2, has been followed for solutions of the labeled chains alone at various initial

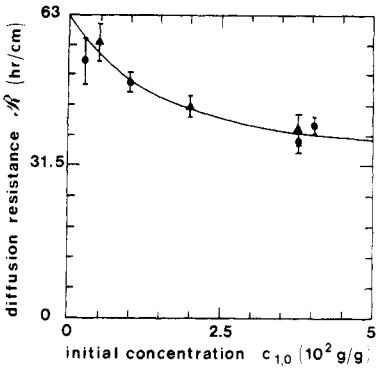

Figure 1. Diffusion resistance of short chains ($m_w = 8.7 \times 10^5$) alone as a function of their initial concentration $c_{1,0}$. Three experiments have been performed with the same cell and membrane for respective values of $c_{1,0}$ of 5×10^{-3} g/g, 10^{-2} g/g, and 3.8×10^{-2} g/g (▲). The other data (●) have been obtained with other cells and membranes. The full line has been calculated from eq 8 as explained in the text.

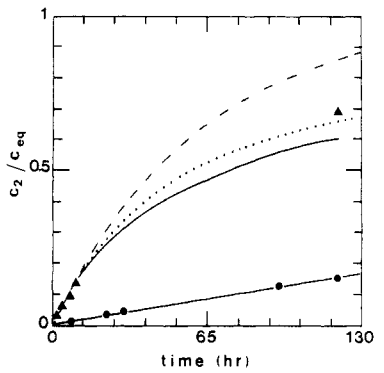

Figure 2. Normalized concentration in compartment 2, c_2/c_{eq}, as a function of time for long chains ($M_w = 6.77 \times 10^6$) alone at two different initial concentrations: 4.85×10^{-3} g/g (●) and 2×10^{-2} g/g (▲). The dashed line is the expected evolution for a diffusion process independent of concentration ($c_2/c_{eq} = 1 - e^{-t/\tau_{eff}}$), with τ_{eff} adjusted from the initial slope. Calculated evolutions with concentration-dependent diffusion rates τ_{eff}^{-1} are also represented. τ_{eff}^{-1} is given by eq 10 for the solid lines and by eq 11 for the dotted line.

Table I
Diffusion Kinetics of Single Species

$c_{1,0}$, g/g	τ_{eff}, h	$\mathcal{R}$, h/cm
$N_p = 8 \times 10^8$; $m_w = 8.7 \times 10^5$		
5×10^{-3}	36.5 ± 1.7	56 ± 4
10^{-2}	31.5 ± 1.5	49 ± 2
3.8×10^{-2}	27 ± 1.5	39 ± 3
$N_p = 2.5 \times 10^8$; $M_w = 7.75 \times 10^5$ [a]		
9.1×10^{-4}		(1.5 ± 0.1) × 10^2

$c_{1,0}$, g/g	$\mathcal{R}$, h/cm	$\mathcal{R}_A$, h/cm	c_A, g/g
$N_p = 8 \times 10^8$; [b] $M_w = 6.77 \times 10^6$			
4.85×10^{-3}	(1 ± 0.1) × 10^3	(1 ± 0.1) × 10^3	(4.5 ± 0.5) × 10^{-3}
2×10^{-2}	(1 ± 0.15) × 10^2	85 ± 15	(1 ± 0.2) × 10^{-2}
$N_p = 2.5 \times 10^8$; [a] $M_w = 6.77 \times 10^6$			
1.1×10^{-3}		>1.5 × 10^4	
4.9×10^{-3}		(4 ± 0.6) × 10^3	(4.5 ± 0.5) × 10^{-3}
7.1×10^{-3}		(9.1 ● 1) × 10^2	(4.5 ± 0.5) × 10^{-3}
1.1×10^{-2}		(2.7 ± 0.3) × 10^2	(4.5 ± 0.5) × 10^{-3}
1.93×10^{-2}		60 ± 15	(4.5 ± 0.5) × 10^{-3}

[a] Results of ref 16. [b] $R_B = (1 \pm 0.15) \times 10^2$ h/cm; $c_B = (4.5 \pm 0.5) \times 10^{-3}$ g/g; $\rho = 3 \pm 2$.

concentrations $c_{1,0}$. The kinetics of diffusion can be fitted to a single-exponential law:

$$c_2/c_{eq} = (1 - e^{-t/\tau_{eff}}) \quad (1)$$

where τ_{eff} is the effective diffusion time through the membrane. The resistance values $\mathcal{R}$ deduced from a best adjustment of eq 1 to the data are plotted in Figure 1 as a function of $c_{1,0}$. Three experiments have been performed with the same cell and membrane; the corresponding resistances are indicated in Figure 1 and are reported in Table I, together with the adjusted values of τ_{eff}. The other data of Figure 1 have been obtained with other cells and membranes in the same range of initial concentration $c_{1,0}$. The reproducibility is comparable to the uncertainty of the determination of the resistance. $\mathcal{R}$ decreases with initial concentration by a factor $^1/_3$ on the explored range: $c_{1,0} = 2.5 \times 10^{-3}$ to 4×10^{-2} g/g.

C. *N* Chains Alone. The kinetics of diffusion of the N chains ($M_w = 6.77 \times 10^6$) are by contrast strongly dependent on their concentration, as previously reported[16] and as evidenced by Figure 2. For $c_{1,0} = 4.85 \times 10^{-3}$ g/g, only a small fraction of the chains diffuses through the membrane, while after comparable times, for $c_{1,0} = 2 \times 10^{-2}$ g/g, c_2 comes much closer to the equilibrium value c_{eq}. Moreover, the kinetics of diffusion for $c_{1,0} = 2 \times 10^{-2}$ g/g slows down as the experiment proceeds and deviates from the simple exponential law (1) represented by the dashed line in Figure 2. The resistance values determined by the initial slope are reported in Table I. $\mathcal{R}$ decreases by a factor 10 in the explored range of concentration.

Discussion

The diffusion kinetics of each type of chains taken alone is a function of the molecular weight and of the initial concentration. We first discuss the dependence of the diffusion resistance on molecular weight in the low concentration limit. Then we examine its concentration dependence.

The results of the present paper can be readily compared to those of ref 16, where similar experiments were conducted under the same conditions, except for the porosity of the filters. The total number of pores N_p of one membrane was 2.5×10^8 in ref 16, instead of 8×10^8 in the present paper. The resistances values are reported in Table I for the two porosities. For comparison with the *n* chains data, we report the resistance obtained in ref 16 with the molecular weight $M_w = 7.75 \times 10^5$ closest to the labeled chain molecular weight $m_w = 8.7 \times 10^5$.

A. Low Concentration Regime. For $c_{1,0} < 5 \times 10^{-3}$ g/g, we observe from Table I that the resistances are inversely proportional to the porosity within experimental uncertainty. This confirms that the contribution of dead layers to the diffusion resistance is negligible for dilute solutions of both types of chains:

$$\mathcal{R} = \mathcal{R}_m$$

The ratio D_{eff}/D_0 can then be estimated as in ref 16 for the two molecular weights in dilute solutions:

$D_{eff}/D_0 \simeq 0.2$ for

$$m_w = 8.7 \times 10^5 \quad \text{and} \quad c_{1,0} < 5 \times 10^{-3} \text{ g/g}$$

$D_{eff}/D_0 < 8 \times 10^{-3}$ for

$$M_w = 6.77 \times 10^6 \quad \text{and} \quad c_{1,0} = 10^{-3} \text{ g/g}$$

In this dilute regime, the chains stay isolated and behave independently. Their diffusion hindrance through the pores D_{eff}/D_0 depends on the parameter $x = R_H/R_p$, ratio of the hydrodynamic radius R_H to the pore radius R_p. The large decrease of D_{eff}/D_0 between the two molecular weights can be attributed to two factors, a static one and

a dynamic one. The static one is the partition coefficient $K(x) = c_p/c$, ratio of the concentration inside the pore to the outside concentration c; it gives the probability for one chain to enter the pore. The dynamic one $f(x)$ is the hydrodynamic drag experienced by the molecules inside the pore.

In a crude description of the chains as hard spheres of radius R_H, these two factors have simple polynomial forms for small x:[6]

$$K_R(x) = (1 - x)^2$$

$$f_R(x) = 1 - 2.1x + 2.1x^3 - 0.95x^5$$

The Renkin equation $D_{eff}/D_0 = K_R(x)f_R(x)$ has been compared to various experimental results obtained with dilute flexible chains[5,15,16] or with more rigid molecules.[3,4b,5] We have found good agreement between the hard-sphere theory and flexible-chain data for $x < 0.4$.[16] However, diffusion of flexible chains has also been reported to be more rapid[5] or slower[15] than predicted by this model. But these discrepancies may probably be attributed[28] to an underevaluation of the pore size[5] or of the boundary layer influence.[15]

For $x \gtrsim 1$ one must take into account the flexibility of the chains.[11,15,16,27] A scaling analysis of Daoud and de Gennes[30] evaluates K for large flexible chains which must become elongated to enter the pore: $K(x) = e^{-x^{5/3}}$. The dynamic factor has been shown by Brochard and de Gennes[31] to be of the form $f(x) = x^{-2/3}$ for chains elongated inside the pore. The scaling law $D_{eff}/D_0 \propto x^{-2/3}e^{-(\alpha x)^{5/3}}$ for $x \gtrsim 1$ and $D_{eff}/D_0 = 1$ for $x \simeq 0$ gives a good description of experimental data when the numerical prefactor α is chosen equal to 2.5.[15,16] This agreement remains, however, somewhat ambiguous, since it is difficult to evaluate D_{eff}/D_0 at $x \gtrsim 1$: the diffusion kinetics becomes extremely slow (characteristic times $>10^4$ h).

B. Concentration Effects. (1) Theoretical Position of the Problem. The effective diffusion coefficient has been already reported to depend drastically on initial concentration for molecular weights of size comparable to or larger than R_p.[16] These molecules are highly excluded from the pores in dilute solutions. The large variation of D_{eff} can be attributed to an increase of the partition coefficient K with $c_{1,0}$. Indeed, Daoudi and Brochard[17] have shown that for a concentrated solution, K should be close to 1. In this regime, the presence of the other chains screens the excluded-volume and hydrodynamic interactions;[18] the screening length ξ is comparable to a monomer size and much smaller than R_p: large chains may then enter the pore without exclusion.

Starting with $K \ll 1$ in a dilute solution and increasing $c_{1,0}$, one should expect that K increases sharply in an intermediate regime of concentration where the chains start to overlap in the outside solution and are still dilute inside the pore. The partition coefficient can be obtained in the same way as in ref 17 by writing the equality of the chemical potentials of one chain isolated and elongated inside the pore and of one chain in the outside solution. The chemical potential of an outside chain increases through the osmotic pressure due to interactions with the other chains. Two approaches are relevant to describe this osmotic potential, depending on the concentration regime in the outside solution. When the chains do not yet overlap but start to be repelled by the excluded volume of others, a virial expansion well describes the osmotic pressure:[32]

$$\Delta\Pi/(RT\rho^2c) = A_2c \qquad (2)$$

where the concentration c is expressed in weight/weight and ρ is the solvent density. A_2 is the second virial coefficient which depends on the solute molecular weight (M_n) as $A_2 \propto M_n^{-0.2}$ in a good solvent. $\Delta\pi$ is the osmotic pressure term describing interactions between two chains. T is the absolute temperature and $R = N_Ak_B$ has the usual meaning. The osmotic potential of one outside chain of N monomers is then of the form $\mu_{os} = k_BTN2A_2m\rho c$, where m is the molar mass of one monomer. With $\alpha = 2A_2m\rho$, the partition coefficient may be written

$$K_N(c_{1,0}) = K_N(c_{1,0}\to 0)e^{N\alpha c_{1,0}} \qquad (3)$$

However, this approach can no longer apply for well-overlapping chains, when the monomer concentration is high enough to be uniform in space. In the semidilute regime, a scaling law for the osmotic pressure has been established by des Cloizeaux:[33]

$$\Delta\Pi M_n/(RT\rho c) = k(c/c^*)^{5/4} \qquad (4)$$

Experimental evidence of this dependence has been reported in various monodisperse polymer solutions by osmometry and light scattering[34-38] for concentrations high enough as compared to the first overlap concentration $c^* = M_n/(4/3\pi R_G^3\rho N_A) \propto N^{-4/5}$. Here M_n is the number-average molecular weight of one chain and R_G its radius of gyration. k is a numerical constant whose order of magnitude has been evaluated theoretically[38] as well as experimentally:[37] $k = 1.5$. Following this approach, we obtain the osmotic potential $\mu_{os} = k_BTk_1(c/c^*)^{5/4}$ and the partition coefficient

$$K_N(c_{1,0}) = K_N(c_{1,0}\to 0)e^{k_1(c_{1,0}/c^*)^{5/4}} \qquad (5)$$

where k_1 is another numerical constant: $k_1 = {}^9/_5k \simeq 2.7$. Equations 2 and 4 have been shown to be in good agreement with osmotic pressure data of flexible chains in good solvent in their respective concentration range, $c \lesssim c^*$ for eq 2 and $c > c^*$ for eq 4.[37]

It is clear that eq 3 and 5 hold only if the concentration inside the pore $c_{1,0}K_N(c_{1,0})$ is low enough that the osmotic potential of one chain inside the pore stays negligible or if the chains stay isolated inside the pore. In this situation, the dynamic factor in D_{eff} is the same as in dilute solutions. Therefore the effective diffusion coefficient of the chains may be written

$$D_{eff}(c_{1,0}) = D_{eff}(c_{1,0}\to 0)e^{N\alpha c_{1,0}} \qquad (6)$$

when the virial expansion is valid and

$$D_{eff}(c_{1,0}) = D_{eff}(c_{1,0}\to 0)e^{k_1(c_{1,0}/c^*)^{5/4}} \qquad (7)$$

for a semidilute solution outside the pore.

The concentration inside the pore is no longer negligible if the chains are smaller than the pore and are not strongly excluded in dilute solutions ($K_N(c_{1,0}\to 0) > 10^{-1}$). Large molecules, even with low values of $K_N(c_{1,0}\to 0)$, are also less and less "dilute" inside the pore as $c_{1,0}$ increases; the range of concentration where eq 3 and 5 apply is nevertheless physically limited by the highest possible value for $K_N(c_{1,0}) = 1$. Therefore it is necessary to extend the previous treatment by taking into account the osmotic potential as well inside the pore. The virial expansion can be used when the chains do not overlap strongly either outside or inside the pore. This situation is practically encountered with small chains or large values of $K_N(c_{1,0}\to 0)$. The partition coefficient is then related to $c_{1,0}$ through

$$K_N(c_{1,0}) = K_N(c_{1,0}\to 0)e^{N\alpha c_{1,0}[1-K_N(c_{1,0})]} \qquad (8)$$

In this regime, the dynamic factor in D_{eff} stays identical

with its value in dilute solutions, since the chains still diffuse independently:

$$D_{eff}(c_{1,0}) = D_{eff}(c_{1,0}\rightarrow 0)e^{Nac_{1,0}[1-K_N(c_{1,0})]} \quad (9)$$

More concentrated regimes where the solution is semidilute outside the pore and more or less concentrated inside have been already theoretically investigated in ref 17. Equations analogous to (8) can be derived for the partition coefficient. When the outside concentration becomes high enough, screening by the other chains should also be of importance inside the pore both for the conformation and the dynamics of the chains. The dynamic factor in D_{eff} should also increase with $c_{1,0}$.

(2) Concentration Regimes. For comparison with the above theoretical models, it is first of importance to examine which concentration regimes have been investigated in terms of $c_{1,0}/c^*$. From ref 37, a one-term virial expansion is no longer valid for $c_{1,0}/c^* > 2$, where c^* is related to A_2 through $c^* = 1/\rho A_2 M_n$. Light scattering data of Munch et al.[19] provide an evaluation of $A_2 = 2 \times 10^{-4}$ mol cm^3 g^{-2} for $M_n = 6.7 \times 10^5$ for polystyrene in ethyl acetate and of the corresponding $c^* = 8.3 \times 10^{-3}$ g/g. However, previous osmometry measurements[20] in the same system show an important disagreement with these data: A_2 is only 7×10^{-5} mol cm^3 g^{-2} for $M_n = 2.4 \times 10^5$ and corresponds to $c^* = 6.6 \times 10^{-2}$ g/g. We may evaluate c^* for our own samples from $c^* \propto M_n^{-4/5}$ (good solvent conditions). From the light scattering data,[19] the first overlap concentration should be for the N chains 1.4×10^{-3} g/g and for the n chains 8.8×10^{-3} g/g, whereas from osmometry,[20] they should be for the N chains 5×10^{-3} g/g and for the n chains 3.1×10^{-2} g/g. In any case, our experiments have then been performed at initial concentrations both below and above c^*.

Literature data also show that the absolute value of c^* is not the same when dynamic properties are involved rather than static ones.[39] More recently, semidilute solutions have been reported to exhibit correlation functions more complex than single exponentials for polystyrene in ethyl acetate[40] as well as in other solvents.[41] The evaluation of a unique correlation length in these solutions then appears as a subject still open to controversy. However, the data of Munch et al.[19] provide an estimation of a crossover concentration for dynamic properties: their dynamic light scattering data exhibit a behavior characteristic of an entangled solution for polystyrene $M_n = 6.7 \times 10^5$ in ethyl acetate for concentrations above 4×10^{-2} g/g. We shall then consider that once the chains have entered the pores, they diffuse as if individually if their concentration inside the pore does not exceed 3×10^{-2} g/g for n chains and 7×10^{-3} g/g for N chains. However, a direct experimental check of the concentration dependence of the friction coefficient of confined flexible chains is still lacking to ascertain the validity of these limits.

(3) *N* Chains (Comparison to Experimental Results). a. Scaling Model. Our previous results obtained with low porosity filters[15] have been shown to be compatible with a diffusion law such as (7). Indeed, we know from the low concentration results that $K_N(c_{1,0}\rightarrow 0) \ll 1$.

The data of Figure 2 can be also compared to this model by using the same fitting procedure as in ref 16; $c_1(t)$ and $c_2(t)$ are calculated point by point with an effective diffusion rate function of $c_1(t)$:

$$\tau_{eff}^{-1}(c_1(t)) = \tau_{dilute}^{-1}e^{(c_1(t)/c_A)^{5/4}} \quad (10)$$

We use here a hypothesis of a quasi-stationary regime of diffusion; the instantaneous diffusion coefficient is only depending on $c_1(t)$ through the partition coefficient at the pore entrance. Two parameters are obtained: c_A is to be compared to $k_1^{-4/5}c^*_M$ in eq 7 and $\mathcal{R}_A$ is the effective diffusion resistance at the beginning of the experiment:

$$\mathcal{R}_A = \tau_{eff}(c_{1,0})(1/V_1 + 1/V_2)S$$

The adjusted curves are represented by full lines in Figure 2. The values of the corresponding c_A and $\mathcal{R}_A$ are reported in Table I, together with those obtained at low porosity.

For $c_{1,0} = 4.85 \times 10^{-3}$ g/g, the data can be described by eq 10. The $\mathcal{R}_A$ values are as expected inversely proportional to the porosity. The c_A value is the same for both porosities. However, we note a discrepancy between the value thus estimated: $c_A = (4.5 \pm 0.5) \times 10^{-3}$ g/g and the theoretical value $k_1^{-4/5}c^*_M$ expected from eq 7, where c^*_M is the first overlap concentration of the N chains evaluated either from static light scattering, $k_1^{-4/5}c^*_M = 6.3 \times 10^{-4}$ g/g, or from osmometry, $k_1^{-4/5}c^*_M = 2.3 \times 10^{-3}$ g/g.

For $c_{1,0} = 2 \times 10^{-2}$ g/g, the data of Figure 2 present smoother kinetics than expected from the low-porosity results. The value of c_A is too high and the resistance $\mathcal{R}_A$ too large as compared to the low-porosity results at the same $c_{1,0}$. These too slow kinetics can be qualitatively understood if the diffusional boundary layer resistance $\mathcal{R}_{bl}$ is taken into account. We assume as a first approximation that the description of the boundary layer effect in dilute solutions[25] is still valuable in semidilute solutions and that $\mathcal{R}_{bl}$ stays of the same order of magnitude during the experiment. However, as $c_1(t)$ decreases, $\rho = 2\mathcal{R}_{bl}/\mathcal{R}_m$ changes drastically through the diffusion hindrance. D_{eff}/D_0 is known to increase by more than 20 when $c_{1,0}$ decreases from 2×10^{-2} to 5×10^{-3} g/g from the results obtained at a porosity $p = 4\%$. With high porosity $p = 14\%$, it is possible that $\rho > 1$ at the beginning of the experiment for $c_{1,0} = 2 \times 10^{-2}$ g/g. We have then adjusted the data to a curve calculated with the same procedure, but with an effective diffusion rate

$$\tau_{eff}^{-1}(c_1(t)) = \tau_{dilute}^{-1}(e^{-(c_1(t)/c_B)^{5/4}} + B)^{-1} \quad (11)$$

The calculated curve depends now on three parameters instead of two: c_B and $\mathcal{R}_B$ have the same meanings as c_A and $\mathcal{R}_A$ above; ρ is estimated at the beginning of the experiment from $\rho = B \exp((c_{1,0}/c_B)^{5/4})$. The values of c_B, $\mathcal{R}_B$, and ρ reported in Table I correspond to the dotted line in Figure 2. The agreement with the data is better when $\tau_{eff}(c_1(t))$ is given by eq 11 than 10. Moreover, the c_B value is identical with the c_A value obtained at low porosity and low concentration. On the other hand, the resistance to diffusion at the beginning of the experiment $\mathcal{R}(c_{1,0})$ is determined from the initial kinetics and does not change with the fitting procedure: $\mathcal{R}(c_{1,0}) \simeq \mathcal{R}_A \simeq \mathcal{R}_B$. It is still too large as compared to the value obtained at $p = 4\%$ and for $c_{1,0} = 2 \times 10^{-2}$ g/g. A possible explanation for this discrepancy is that $\mathcal{R}_{bl}$ also depends on concentration and porosity, contrary to the simple assumptions used in (11). Careful experimental investigations still seem necessary to elucidate this point. ρ as evaluated from (11) should be nonnegligible at the beginning of the experiment.

This analysis of the data shows that with high-porosity filters and at high initial concentration the diffusion boundary layers contribute to the effective diffusion resistance and limits the accuracy on the determination of $\mathcal{R}_m$ at the beginning of the experiment. A diffusion law such as (11) is probably too schematic to describe $\mathcal{R}_{bl}$ during the whole experiment. But it enables one to evaluate physical parameters consistent with these obtained at lower ρ, i.e., at lower porosity p. Therefore all our results on the N chain diffusion are compatible with the same model: the acceleration of the N chains diffusion can be described as due to an increase of their partition coefficient K_N with $c_{1,0}$. When this approach is used, the discrepancy between the adjusted parameter $c_A = (4.5 \pm$

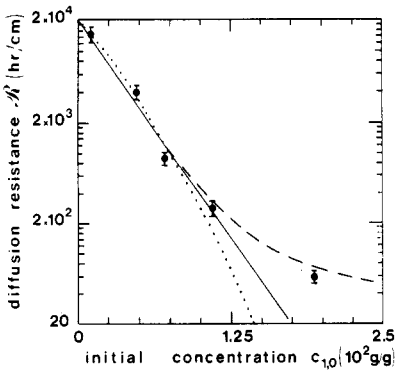

Figure 3. Long chain diffusion resistance as a function of initial concentration $c_{1,0}$ from the data of ref 16. Two models predict a large increase of the partition coefficient K_N with $c_{1,0}$ which explain the observed acceleration of the diffusion: the full line has been calculated from a simple virial expansion (eq 12 with $c_v = 2.5 \times 10^{-3}$ g/g), while the dotted line is derived from scaling arguments (eq 10 with $c_A = 3.1 \times 10^{-3}$ g/g). The deviation from these laws at $c_{1,0} = 2 \times 10^{-2}$ g/g may be interpreted as their higher limit of validity, when $K_N(c_{1,0})$ becomes too large; the dashed line calculated from eq 8 as explained in the text better agrees with all the data.

$0.5) \times 10^{-3}$ g/g and its theoretical evaluation $k_1^{-4/5}c^*_M$ remains unclear.

b. Virial Expansion. Our data cannot yet provide a clear-cut confirmation of the scaling law (4) for the osmotic pressure. Equally good fits to the data of ref 16 and of this paper are obtained by comparing them to a virial expansion equation such as (6) and by taking for the effective (instantaneous) diffusion rate through the membrane, with the same hypothesis of a quasi-stationary regime of diffusion as in eq 10:

$$\tau_{\text{eff}}^{-1}(c_1(t)) = \tau_{\text{dilute}}^{-1} e^{(c_1(t)/c_v)} \qquad (12)$$

New sets of parameters c_v and $\mathcal{R}_v$ are obtained. As already noticed, the effective diffusion resistance at the beginning of the experiment $\mathcal{R}(c_{1,0})$ is determined experimentally and does not change with the fitting procedure: $\mathcal{R}_{(1,0)} = \mathcal{R}_A = \mathcal{R}_v$. c_v is to be identified in eq 6 to $(N\alpha)^{-1} = (2M_nA_2\rho)^{-1}$. It has the same value for all the experiments: $c_v = (2.5 \pm 0.2) \times 10^{-3}$ g/g. It corresponds to a virial coefficient $A_2 = 3.7 \times 10^{-5}$ mol cm^3 g^{-2}.

This is too small as compared to Munch et al.[19] light-scattering data, but in fair agreement with the osmometry[20] determination.

c. Comparison between the Two Approaches. The scaling law for the osmotic pressure (4) should differ significantly from the virial expansion (2) at high enough concentrations. Our data stay compatible with both approaches for two reasons: (i) the explored concentration range is only $c_{1,0} = c^*_M/3.5$ up to $c_{1,0} = 4c^*_M$ if we take $c^*_M = 5 \times 10^{-3}$ g/g as suggested by the good agreement between the adjusted parameter from the virial expansion model c_v and the osmometry data. Differences between the two models should only appear for $c_{1,0} = 2 \times 10^{-2}$ g/g, at the highest investigated concentration; (ii) this concentration probably corresponds to the higher limit of validity of eq 3 and 5 when K becomes larger than 10^{-1}. We have reported in Figure 3 the experimental results $\mathcal{R}(c_{1,0})$ of ref 16 as a function of $c_{1,0}$. Theoretical curves are also represented. The full lines corresponds to eq 12 with $c_v = 2.5 \times 10^{-3}$ g/g, and the dotted line to eq 10 with $c_A = 3.1 \times 10^{-3}$ g/g. Both curves have been calculated with $\mathcal{R}(c_{1,0}=0) = 2 \times 10^4$ h/cm. It is clear that the agreement with the data is as good with either of the theoretical curves up to $c_{1,0} = 10^{-2}$ g/g. At $c_{1,0} = 2 \times 10^{-2}$ g/g, the resistance obtained is 1 order of magnitude higher than it is with both laws. This could reflect the fact that $\mathcal{R}_{bl}$ is no longer negligible, as previously discussed. But it can also be interpreted as the higher limit of validity of eq 3 and 5, when the concentration inside the pore is no longer negligible. We have calculated $K_N(c_{1,0})$ from eq 8 with $(N\alpha)^{-1} = c_v = 2.5 \times 10^{-3}$ g/g and deduced $\mathcal{R}(c_{1,0}) = \mathcal{R}(c_{1,0}=0)[K_N(c_{1,0}=0)/K_N(c_{1,0})]$, for a given value of $K_N(c_{1,0}=0)$. $\mathcal{R}(c_{1,0})$ thus calculated is represented by a dashed line in Figure 3. It is in agreement with the data on the whole range of $c_{1,0}$ for $K_N(c_{1,0}=0) = 10^{-3}$ and $\mathcal{R}(c_{1,0}=0) = 2 \times 10^4$ h/cm. It also enables estimation of $K_N(c_{1,0}=2\times10^{-2}\text{g/g}) = 0.33$. The concentration inside the pore should then never exceed 7×10^{-3} g/g, a higher concentration for which the N chains may be considered as diffusing independently inside the pore.

(4) *n* Chains (Comparison to Experimental Results). The partition coefficient of the n chains from the pores in dilute solution is given by steric exclusion, since they are smaller than the pore size: $x = R_H/R_p = 0.3$ and $K_n(c_{1,0}\to0) = 0.5$. Because of such a moderate exclusion, there is not a strong concentration difference between the pore and the outside solution. Therefore $K_n(c_{1,0})$ should not be strongly concentration dependent, and it must be evaluated by eq 8. From the analysis of the N chain results, we know that in the concentration regime of the n chain experiments, the virial expansion should be valid: $c_{1,0}$ varies between $c^*_m/10$ up to $1.3c^*_m$ with $c^*_m = c^*_M(M_n/m_n)^{+4/5} = 3 \times 10^{-3}$ g/g. If the dynamic factor in D_{eff} stays constant in this regime, the decrease of $\mathcal{R}$ with $c_{1,0}$ is only due to the increase of $K_n(c_{1,0})$. Indeed, the results of Figure 1 are in agreement with such a model. The full line represents $\mathcal{R}(c_{1,0}) = \mathcal{R}(c_{1,0}=0)[K_n(c_{1,0}=0)/K_n(c_{1,0})]$ with $\mathcal{R}(c_{1,0}=0) = 63$ h/cm and where $K_n(c_{1,0})$ has been calculated by eq 8 with $K_n(c_{1,0}=0) = 0.5$ and $(n\alpha)^{-1} = 1.5 \times 10^{-2}$ g/g. It corresponds to a virial coefficient $A_2 = 5.8 \times 10^{-5}$ mol cm^3 g^{-2}. This value agrees with the value of A_2 obtained for the N chains when a scaling law for A_2: $A_2 \propto M_n^{-0.2}$ is used. We can also check that for $c_{1,0} = 4 \times 10^{-2}$ g/g, the concentration inside the pore does not exceed 3.3×10^{-2} g/g: it is consistent with the hypothesis that the dynamic factor in D_{eff} is the same as for isolated chains.

Conclusion

The diffusion kinetics of polymer solutions through model porous membranes of pore radius $R_P = 75$ nm has been investigated as a function of concentration. The observed aceleration of diffusion can be attributed to the same mechanism, an increase of the partition coefficient from the pores with concentration for the two molecular weights investigated. A simple virial expansion of the osmotic pressure takes into account the results. The relevant concentration parameter c_v is related to the virial coefficient A_2 through $c_v = 1/2\rho A_2 M_n$, where M_n is the number-average molecular weight and ρ the solvent density. We obtain A_2 values in good agreement with evaluations from independent osmometry experiments. For small molecules not strongly excluded from the pores in dilute solutions, the concentration dependence observed is not very large. The confirmation of the model remains qualitative. For large molecules, the effect of concentration is drastic and demonstrates the role of the flexibility of the chains: long chains are strongly excluded from the pores in dilute solutions but their partition coefficient changes by more than 2 orders of magnitude on a 4-fold increase of concentration. The results can be equally well described by a variation of the osmotic pressure following a virial expansion or a scaling law. Differences between the two laws cannot be easily observed, since they should only appear at the upper limit of the concentration regime

where the partition coefficient becomes comparable to 1 and is less and less sensitive to concentration. For a more definite confirmation of this point, it should be necessary to perform experiments at higher R_H/R_p value.

The presence of the diffusional boundary layer limits the accuracy of the determination of the true diffusion coefficient through the membrane. Its influence is minimized at low porosity at the cost of longer duration of the diffusion experiments.

Registry No. Polystyrene, 9003-53-6; bisphenol A polycarbonate (copolymer), 25037-45-0; bisphenol A polycarbonate (SRU), 24936-68-3.

References and Notes

(1) Satterfield, C. N.; Colton, C. K.; Pitcher, W. H. *AIChE J.* **1975**, *21*, 289.
(2) Haller, W. *Macromolecules* **1977**, *10*, 83.
(3) Beck, R. E.; Schulz, S. J. *Biochim. Biophys. Acta* **1972**, *255*, 273.
(4) (a) Long, T. D.; Jacobs, D. L.; Anderson, J. L. *J. Membr. Sci.* **1981**, *9*, 13. (b) Baltus, R. E.; Anderson, J. L. *Chem. Eng. Sci.* **1983**, *38*, 1959.
(5) Bohrer, M. P.; Patterson, G. D.; Carroll, P. J. *Macromolecules* **1984**, *17*, 1170.
(6) Renkin, E. M. *J. Gen. Physiol.* **1954**, *38*, 225.
(7) Bean, C. P. In *Membranes, A Series of Advances*; Eisenman, G., Ed.; Wiley: New York, 1972, Vol. 1.
(8) Giddings, J. C.; Kucera, E.; Russell, C. P.; Myers, M. N. *J. Phys. Chem.* **1968**, *72*, 4397.
(9) Anderson, J. L.; Quinn, J. A. *Biophys. J.* **1974**, *14*, 130.
(10) (a) Casassa, E. F. *J. Polym. Sci., Part B* **1967**, *5*, 773. (b) Casassa, E. F.; Tagami, Y. *Macromolecules* **1969**, *2*, 14. (c) Casassa, E. F. *Macromolecules* **1976**, *9*, 182.
(11) Satterfield, C. N.; Colton, C. K.; de Turckeim, B.; Copeland, T. M. *AIChE J.* **1978**, *24*, 937.
(12) Schulz, J. S.; Valentine, R.; Choi, C. Y. *J. Gen. Physiol.* **1979**, *73*, 49.
(13) Long, T. D.; Anderson, J. L. *J. Polym. Sci., Polym. Phys. Ed.* **1984**, *22*, 1261.
(14) (a) Chauveteau, G.; Tirrell, M.; Omari, A. *J. Colloid Interface Sci.* **1984**, *100*, 41. (b) Nguyen, Q., T.; Néel, J. *J. Membr. Sci.* **1983**, *14*, 97, 111.
(15) Cannell, D.; Rondelez, F. *Macromolecules* **1980**, *13*, 1599.
(16) Guillot, G.; Léger, L.; Rondelez, F. *Macromolecules* **1985**, *18*, 2531.
(17) Daoudi, S.; Brochard, F. *Macromolecules* **1978**, *11*, 751.
(18) De Gennes, P.-G. In *Scaling Concepts in Polymer Physics*; Cornell University: Ithaca, NY, 1979.
(19) Munch, J. P.; Candau, S.; Herz, J.; Hild, G. *J. Phys. (Les Ulis, Fr.)* **1977**, *38*, 971.
(20) (a) Schick, M. J.; Doty, P.; Zimm, B. H. *J. Am. Chem. Soc.* **1950**, *72*, 530. (b) Jacobsson, G. *Acta Chem. Scand.* **1954**, *8*, 1843. (c) Vink, H. *Eur. Polym. J.* **1974**, *10*, 149.
(21) Guillot, G. *Macromolecules*, following paper in this issue.
(22) Guillot, G.; Rondelez, F. *J. Appl. Phys.* **1981**, *52*, 7155.
(23) Léger, L.; Hervet, H.; Rondelez, F. *Macromolecules* **1981**, *14*, 1732.
(24) Lesec, J. Ecole Supérieure de Physique et Chimie, Paris, private communication.
(25) (a) Malone, D. M.; Anderson, J. L. *AIChE J.* **1977**, *23*, 177. (b) Keller, K. H.; Stein, T. T. *Math. Biosci.* **1967**, *1*, 421.
(26) (a) Odell, J. A.; Keller, A.; Miles, M. J. *Polym. Commun.* **1983**, *24*, 7. (b) Munch, W. D.; Zestar, L. P.; Anderson, J. L. *J. Membr. Sci.* **1979**, *77*, 102.
(27) Bohrer, M. P. *Ind. Eng. Chem. Fundam.* **1983**, *22*, 72.
(28) Guillot, G. Thèse Université Paris-Sud, Orsay, 1986.
(29) Zemans, L.; Wales, M. *Sep. Sci. Technol.* **1981**, *16*, 275.
(30) Daoud, M.; de Gennes, P. G. *J. Phys. (Les Ulis, Fr.)* **1977**, *38*, 85.
(31) Brochard, F.; de Gennes, P.-G. *J. Chem. Phys.* **1977**, *67*, 52.
(32) (a) Flory, P. J. *Principles of Polymer Chemistry*; Cornell University Press: Ithaca, NY, 1978. (b) Tanford, C. *Physical Chemistry of Macromolecules*; Wiley: New York, 1968.
(33) Des Cloizeaux, J. *J. Phys. (Les Ulis, Fr.)* **1975**, *36*, 281.
(34) Daoud, M.; Cotton, J. P.; Farnoux, B.; Jannink, G.; Sarma, G.; Benoît, H.; Duplessix, R.; Picot, C.; de Gennes, P.-G. *Macromolecules* **1975**, *8*, 804.
(35) Candau, F.; Strazielle, S.; Benoît, H. *Eur. Polym. J.* **1976**, *12*, 95.
(36) Roots, J.; Nystrom, B. *Polymer* **1979**, *20*, 148.
(37) Noda, I.; Kato, N.; Kitano, T.; Nagasawa, M. *Macromolecules* **1981**, *14*, 668.
(38) Des Cloizeaux, J.; Noda, I. *Macromolecules* **1982**, *15*, 1505.
(39) (a) Adam, M.; Delsanti, M. *J. Phys. (Les Ulis, Fr.)* **1980**, *41*, 713. (b) Wilzius, P.; Haller, H. R.; Cannell, D.; Schaeffer *Phys. Rev. Lett.* **1984**, *53*, 834.
(40) Brown, W. *Macromolecules* **1986**, *19*, 1083.
(41) Brown, W. *Macromolecules* **1985**, *18*, 1713 and references therein.

Diffusion of Polystyrene Solutions through Model Membranes. 2. Experiments with Mixture Solutions

G. Guillot

Physique de la Matière Condensée† Collège de France, 75231 Paris Cedex 05, France.

Received June 27, 1986

ABSTRACT: The diffusion of bimodal solutions of polystyrene molecules through model porous membranes of pore radius R_p = 75 nm has been examined as a function of the polymer concentration and of the solution composition in long and short chains. With mixtures of long and short chains, we have obtained two new results by analyzing the composition of the solutions after passage through the membrane: (1) In a dilute concentration regime, the long chains stay blocked by the membrane, but the short chains experience an expulsion through the membrane; it can be interpreted as an osmotic expulsion due to the retention of the long chains. (2) The transport of the long chains through the membrane is also accelerated when the number of long chains is kept constant and the concentration is increased by the addition of short chains above the overlap concentration of short chains c_m*. This enhanced diffusion may be attributed to the increase of the long-chain partition coefficient in the presence of short chains. The results are in qualitative agreement with a simple virial expansion model where the same parameters are used as in the analysis of single-chain diffusion kinetics.[1]

Introduction

Solute transport in porous media is generally considered to be controlled by the size of the solute as compared to the pore size. This behavior is well corroborated by a variety of experiments as well as theoretically for solutes small compared to the pore size (see ref 1–9 of the accompanying paper[1]). However, long flexible chains have been observed to enter into pores smaller than their hydrodynamic radius when either the concentration[1-5] or the flow rate[6,7] is increased. Simple scaling arguments[8,9] show that in the absence of flow, long flexible chains should

† Unité Associée au CNRS (U.A. 792).

0024-9297/87/2220-2606$01.50/0